



HAL
open science

Acoustic absorption and generation in varying area ducts with non-isentropic mean flow

Saikumar Reddy Yeddula, R Gaudron, Aimee S. Morgans

► **To cite this version:**

Saikumar Reddy Yeddula, R Gaudron, Aimee S. Morgans. Acoustic absorption and generation in varying area ducts with non-isentropic mean flow. eForum Acusticum 2020, Dec 2020, Lyon, France. pp.785-790. hal-03229440

HAL Id: hal-03229440

<https://hal.science/hal-03229440v1>

Submitted on 21 May 2021

HAL is a multi-disciplinary open access archive for the deposit and dissemination of scientific research documents, whether they are published or not. The documents may come from teaching and research institutions in France or abroad, or from public or private research centers.

L'archive ouverte pluridisciplinaire **HAL**, est destinée au dépôt et à la diffusion de documents scientifiques de niveau recherche, publiés ou non, émanant des établissements d'enseignement et de recherche français ou étrangers, des laboratoires publics ou privés.

ACOUSTIC ABSORPTION AND GENERATION IN VARYING AREA DUCTS WITH NON-ISENTROPIC MEAN FLOW

Saikumar R. Yeddula¹

Renaud Gaudron¹

Aimee S. Morgans¹

¹Department of Mechanical Engineering, Imperial College London, United Kingdom

s.yeddula18@imperial.ac.uk, r.gaudron@imperial.ac.uk

ABSTRACT

Varying area ducts which sustain both subsonic mean flow and temperature gradients are found in engineering applications like combustors, automotive exhaust systems, and boilers. The axially varying flow conditions affect the acoustic energy balance of the system and are crucial for understanding thermo-acoustic oscillations in combustors. For example, the acoustic energy absorbed or generated can be controlled by the amount of heat transfer from the duct. The objective of this work is to present a simple model to estimate the acoustic energy absorption coefficient, Δ , in a varying area duct with a non-isentropic mean flow. A numerical methodology is discussed for calculating Δ . The acoustic-entropy coupling is neglected in the current analysis as the considered flow Mach numbers are $\ll 1$. A semi-analytical solution from a previous work is then used to predict the Δ - leading to an analytical expression. The analytical model when applied to a conical duct with linear temperature gradient, it was found to be accurate when the average of upstream and downstream Mach numbers are less than ~ 0.25 . A parametric analysis revealed that in these low Mach number regimes, the effect of the temperature gradient influences Δ more strongly than the area variation. The results were also independent of Helmholtz number, provided the lower frequency limit for the semi-analytical solution is satisfied.

1. INTRODUCTION

Ducts with varying area, axial temperature gradients and a non-zero subsonic mean flow are often encountered in applications involving flow of hot gases, ranging from automotive exhaust systems to aero-engine combustors [1,2]. These temperature and area gradients impact the acoustic energy balance of the system [3]. The main objective of this work is to analytically estimate the acoustic energy absorption coefficient in such ducts (shown in Fig. (1)). A simplified expression also aids in the parametric analysis aimed at identifying regions of maximum acoustic energy absorption or generation.

Current analysis assumes that the acoustic wave fronts are planar 1-D waves and terms with flow Mach number of order $O(M^3)$ and higher are neglected. This is a reasonable assumption as combustors require low Mach number flows, typically around 0.2, to keep the flame attached. Also, gas Mach numbers in the exhaust manifold of the

automobiles are around ~ 0.15 to have increased reaction time in the catalytic converter [4]. WKB method based semi-analytical solution is used in deriving the analytical expression for Δ . These solutions assume frequencies to be sufficiently large that the WKB methods can be used, yet sufficiently low that higher-order acoustic modes are not cut-on. The acoustic-entropy coupling effect can thereby be neglected as the flow Mach numbers are low [5] and significant turbulent shear dispersion of the entropy wave observed at the considered high frequencies [6].

Further sections are organized as follows. For non-isentropic flows, in Section 2 a procedure for solving the linearised Euler equations and thereby obtain the Δ is presented. In Section 3 the wave amplitudes are estimated using the semi-analytical solution of Yeddula and Morgans [7], and there-by an expression for analytical estimate of Δ is presented. For a conical duct with a linear temperature gradient, the analytical solution is applied and this is discussed in Section 4. In Section 5, the analytical estimates of Δ for different flow configurations, frequencies are compared to numerical results. Conclusions are drawn in the final Section.

2. PROBLEM FORMULATION

In ducts sustaining both area variation and non-isentropic mean flow, the mean flow can be considered one-dimensional (quasi 1D mean flow) when the variations in the radial direction associated to boundary layer growth are negligible. The conservation equations for one-dimensional perfect inviscid flow in such a duct with a changing cross-sectional area change along with mean temperature variation are as follows:

• Mass conservation

$$A \frac{\partial \rho}{\partial t} + \frac{\partial(\rho Au)}{\partial x} = 0 \quad (1)$$

• Momentum conservation

$$\frac{\partial u}{\partial t} + u \frac{\partial u}{\partial x} + \frac{1}{\rho} \frac{\partial p}{\partial x} = 0 \quad (2)$$

• Energy conservation and equation of state

$$\frac{\partial s}{\partial t} + u \frac{\partial s}{\partial x} = \frac{R_g}{p} \dot{Q} \quad \text{and} \quad p = \rho R_g T \quad (3, 4)$$

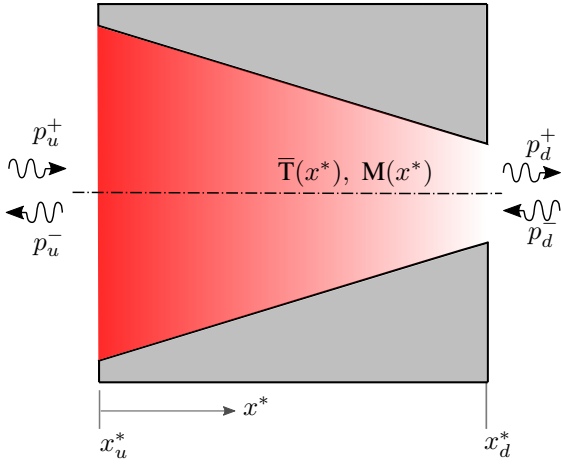


Figure 1: Varying area duct sustaining non-isentropic mean flow. p^\pm and $\hat{\epsilon}$ represent the acoustic and entropy planar wave components. x^* represents the x-coordinate, normalised with length of the duct, l .

where ρ, p, T, u, s, R_g , denote density, pressure, temperature, axial velocity, entropy and universal gas-constant respectively. It is assumed that there are no heat-fluctuations $\dot{Q}^l = 0$; and R_g, γ (the ratio of the specific heats) as constants with values of $287 \text{ Jkg}^{-1}\text{K}^{-1}$ and 1.4 respectively.

The area and mean-temperature gradients of the duct are normalised according to:

$$\alpha^* = \frac{1}{A} \frac{dA}{dx^*}; \quad \beta^* = \frac{1}{\bar{T}} \frac{d\bar{T}}{dx^*}. \quad (5, 6)$$

On expressing the pressure and velocity fluctuations in terms of positive (+) and negative (-) direction propagating wave amplitudes [5], as,

$$\hat{p} = p^+ + p^-, \quad \hat{u} = \frac{1}{\bar{\rho} \bar{c}} (p^+ - p^-), \quad \hat{\epsilon} = \gamma \bar{p} \hat{\sigma}, \quad (7)$$

the linearised equations are recast into a first order system of differential equations for acoustic and entropy wave amplitudes, given by,

$$\begin{aligned} \frac{dp^\pm}{dx^*} = & p^+ \left[\overbrace{\left[\frac{-1}{2(1 \pm M)} \left(\mathcal{K}_1 + \frac{1}{\bar{\rho} \bar{c}} \mathcal{K}_2 + \frac{d}{dx} \left(\frac{1}{\bar{\rho} \bar{c}} \mathcal{K}_3 \right) \right) \right]}^{C_{11} \text{ (or) } C_{21}} \right] \\ & + p^- \left[\overbrace{\left[\frac{-1}{2(1 \pm M)} \left(\mathcal{K}_1 - \frac{1}{\bar{\rho} \bar{c}} \mathcal{K}_2 - \frac{d}{dx} \left(\frac{1}{\bar{\rho} \bar{c}} \mathcal{K}_3 \right) \right) \right]}^{C_{12} \text{ (or) } C_{22}} \right] \\ & + \hat{\epsilon} \left[\overbrace{\left[\frac{M^2}{2(1 \pm M)} \frac{1}{\bar{u}} \frac{d\bar{u}}{dx} \right]}^{C_{13} \text{ (or) } C_{23}} \right], \end{aligned} \quad (8)$$

where,

$$\mathcal{K}_1 = D \pm AM, \quad \mathcal{K}_2 = E \pm BM, \quad \mathcal{K}_3 = F \pm CM.$$

$$\begin{aligned} \frac{d\hat{\epsilon}}{dx} = & p^+ \left[\overbrace{\left[\zeta \left(\gamma + \frac{1}{M} \right) \right]}^{C_{31}} \right] + p^- \left[\overbrace{\left[\zeta \left(\gamma - \frac{1}{M} \right) \right]}^{C_{32}} \right] \\ & - \hat{\epsilon} \left[\overbrace{\left[\frac{iHe}{M} - \frac{1}{\bar{p}} \frac{d\bar{p}}{dx} \right]}^{C_{33}} \right]; \end{aligned} \quad (9)$$

where,

$$\zeta = \left(\frac{\alpha^* M^2 (\gamma - 1) - \beta^* (1 - M^2)}{1 - \gamma M^2} \right)$$

The above equations represent the general form of linearised Euler equations in 1D without neglecting the effect of acoustic-entropy coupling. They can be represented in a simple matrix notation as,

$$\mathbf{W}'(x^*) = \mathbf{C}_{3 \times 3} \mathbf{W}(x^*); \quad \text{and } \mathbf{C} = \begin{bmatrix} C_{11} & C_{12} & C_{13} \\ C_{21} & C_{22} & C_{23} \\ C_{31} & C_{32} & C_{33} \end{bmatrix} \quad (10)$$

and, $\mathbf{W}(x^*) = [p^+(x^*) \quad p^-(x^*) \quad \hat{\epsilon}(x^*)]^T$. In the above equation, the prime (') denotes differentiation with respect to x^* . The elements of the coefficient matrix, $\mathbf{C}_{3 \times 3}$ are given as denoted in Eqs. (8) and (9).

Eq. (10) represents a system of first order differential equations that are solved using Runge-Kutta fourth order scheme for the general solution of acoustic and entropy wave components, p^\pm and $\hat{\epsilon}$ respectively. However, it can be observed from Eq. (8) that the coefficient of $\hat{\epsilon}$ is of the order $O(M^2)$ and hence negligible, given the low Mach number assumption [5]. Further, as stated earlier, the current analysis is aimed at high frequencies for the analytical solutions based on WKB method to be applicable. At these frequencies the entropy waves are subjected to significant shear dispersion, resulting in the attenuation of their wave amplitudes [6]. Hence, we decouple the effect of entropy propagation and only consider the acoustic response of the element to incoming acoustic waves, independent of entropy waves, and there-by solve for for p^\pm . The acoustic wave amplitudes at x_u^*, x_d^* are related by the definition of transfer matrix $\mathbf{T}_{2 \times 2}$, as follows,

$$\mathbf{G}(x_d^*) = [\mathbf{T}]_{2 \times 2} \mathbf{G}(x_u^*); \quad \text{where } \mathbf{G}(x^*) = \begin{bmatrix} p^+(x^*) \\ p^-(x^*) \end{bmatrix} \quad (11)$$

On representing the positive (+) and negative (-) directed propagating wave amplitudes at x_u^* and x_d^* as p_u^\pm and p_d^\pm , the acoustic absorption coefficient (Δ), in the presence of mean flow was shown in [8,9] as,

$$\Delta = 1 - \frac{(1 + M_d)^2 |p_d^+|^2 + \theta \Xi \xi^{-1} (1 - M_u)^2 |p_u^-|^2}{\theta \Xi \xi^{-1} (1 + M_u)^2 |p_u^+|^2 + (1 - M_d)^2 |p_d^-|^2} \quad (12)$$

where, $\theta = A_u/A_d$; A_u, M_u, A_d, M_d correspond to duct area and Mach numbers at x_u^* and x_d^* respectively. Ξ, ξ are the ratio of mean speed of sounds and mean-pressure at duct inlet to outlet, ($\Xi = \sqrt{\bar{T}_u/\bar{T}_d}$, and $\xi = \bar{p}_u/\bar{p}_d$).

For any given arbitrary area, temperature profiles, the mean flow is solved to determine Mach number distribution and ζ . On establishing the mean flow solution, the first order system of differential equations given by Eq. (8) are solved for different upstream boundary conditions. As the problem is linear, the elements of the Transfer matrix are determined using different boundary conditions. Eq. (11), then gives p_d^\pm for given p_u^\pm , and from Eq. (12) corresponding acoustic energy absorption coefficient, Δ , is calculated. Δ can also be evaluated analytically using p_d^\pm from existing approximate analytical solutions. This analysis is described in Section 3.

3. ANALYTICAL EXPRESSION FOR ACOUSTIC ABSORPTION COEFFICIENT

For varying area ducts sustaining non-isentropic mean flow, a semi-analytical solution was presented in [7], in terms of positive (+) and negative (-) direction propagating planar wave amplitudes. Using the principle of superposition, the overall analytical solution for the pressure was expressed in their work as,

$$\begin{aligned}\hat{p}(x^*, \omega) &= C^+ \mathcal{P}^+(x^*, \omega) + C^- \mathcal{P}^-(x^*, \omega), \\ \hat{u}(x^*, \omega) &= \frac{1}{\rho c} (\mathcal{B}^+ C^+ \mathcal{P}^+ - \mathcal{B}^- C^- \mathcal{P}^-),\end{aligned}\quad (13)$$

with C^\pm as constants determined from boundary conditions, and,

$$\begin{aligned}\mathcal{P}^\pm &= \left(\frac{A_1}{A}\right)^{1/2} \left(\frac{T_1}{T}\right)^{1/4} \exp\left(\int_{x_1^*}^{x^*} i \left(\frac{\mp \text{He}}{1 \pm M} \pm \frac{\Phi_{NI}^\pm}{2\text{He}}\right) d\check{x}\right) \\ &\times \left[\frac{\exp\left(\frac{M^2}{2} \mp M + \frac{\gamma}{2} \int_{x_1^*}^{x^*} (\alpha^* M^2 \mp \beta^* M) d\check{x}\right)}{\exp\left(\frac{M_1^2}{2} \mp M_1\right)} \right],\end{aligned}\quad (14)$$

$$\begin{aligned}\mathcal{B}^\pm &= \frac{1}{\mathcal{J}_1} \left[i\text{He} (1 - \gamma M^2) \pm \frac{\beta^*}{4} \pm \frac{\alpha^*}{2} - \alpha^* M + \right. \\ &\left. \frac{\beta^* M}{2} (1 + \gamma) \pm \frac{\beta^* M^2}{4} (3\gamma - 7) \pm \frac{\alpha^* M^2}{2} (3 - 2\gamma) \right].\end{aligned}\quad (15)$$

with $\mathcal{J}_1 = i\text{He} (1 - \gamma M^2) + (\beta^* - 2\alpha^*) M$. The expression for Φ_{NI}^\pm in Eq. (14) is given by,

$$\begin{aligned}\frac{\Phi_{NI}^\pm}{\text{He}^2} &= \frac{1}{\text{He}^2} \left[\frac{\alpha^2}{4} + \frac{3\beta^2}{16} + \frac{\alpha\beta}{2} + \frac{1}{2} \frac{d\beta}{dx} \left(\frac{1}{2} \pm M(\gamma - 1) \right) \right. \\ &\left. + \frac{d\alpha}{dx} \left(\frac{1}{2} \pm M \right) \mp M \left(\alpha^2 + \frac{\beta^2}{2} (1 - \gamma) - \frac{\alpha\beta}{2} (3 - \gamma) \right) \right].\end{aligned}\quad (16)$$

On comparing Eqs. (7) and (13), and defining upstream

reflection coefficient as $R_u = p_u^+ / p_u^-$, we arrive at,

$$\begin{aligned}\frac{C^\pm}{p_u^-} &= \frac{2 \left[\frac{R_u}{1 \mp \mathcal{B}_u^\mp} - \frac{1}{1 \pm \mathcal{B}_u^\mp} \right]}{\left[\frac{1 \pm \mathcal{B}_u^\pm}{1 \mp \mathcal{B}_u^\mp} - \frac{1 \mp \mathcal{B}_u^\pm}{1 \pm \mathcal{B}_u^\mp} \right]}, \\ p_d^\pm &= C^+ \mathcal{P}_d^+ (1 \pm \mathcal{B}_d^+) + C^- \mathcal{P}_d^- (1 \mp \mathcal{B}_d^-),\end{aligned}$$

where, \mathcal{B}_u^\pm and \mathcal{B}_d^\pm are the values of the expression Eq. (15) (corresponding to positive (+) or negative (-) directed propagating wave amplitudes) at x_u^* and x_d^* respectively. Thus, again using Eq. (12), the acoustic absorption coefficient Δ is calculated with analytically determined p_d^\pm (from Eq. (18)).

4. VALIDATION

Although the analysis can in general be applied to ducts of any shape and any mean-temperature distribution, (provided $\frac{\Phi_{NI}^\pm}{\text{He}^2} \ll 1$), a conical test case (shown in Fig. (1)) with a linear temperature gradient is considered for validation. For such a configuration, a fully analytical solution is presented in [7] by further evaluating the integrals in Eq. (14) (the readers are suggested to refer this article for complete solution).

For the conical duct with linear temperature gradient shown in Fig. (1), with radius r_u and temperature \bar{T}_u at x_u^* , radius r_d and temperature \bar{T}_d at x_d^* ,

$$\begin{aligned}A(x^*) &= \pi r_u^2 (1 + a^* x^*)^2, \quad \bar{T}(x^*) = \bar{T}_1 (1 + b^* x^*); \\ \text{where } a^* &= \frac{r_d - r_u}{r_u}, \quad b^* = \frac{\bar{T}_d - \bar{T}_u}{\bar{T}_u}.\end{aligned}\quad (19a-d)$$

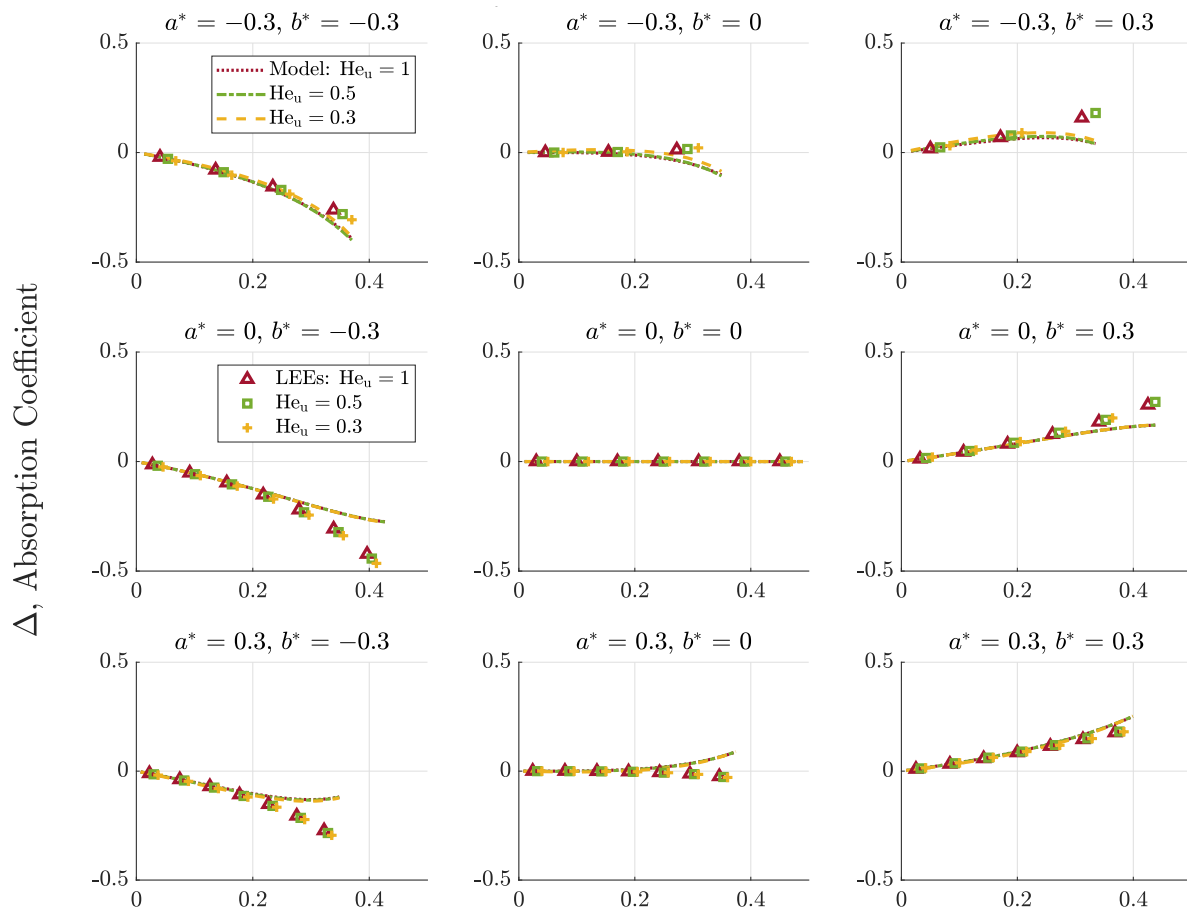
Thus area and temperature gradient parameters, α^* , β^* , and corresponding spatial derivatives become,

$$\begin{aligned}\alpha^* &= \frac{1}{A} \frac{dA}{dx^*} = \frac{2a^*}{(1 + a^* x^*)} \Rightarrow \frac{d\alpha^*}{dx^*} = -\frac{\alpha^{*2}}{2}; \\ \beta^* &= \frac{1}{\bar{T}} \frac{d\bar{T}}{dx^*} = \frac{b^*}{(1 + b^* x^*)} \Rightarrow \frac{d\beta^*}{dx^*} = -\beta^{*2}.\end{aligned}\quad (20a-d)$$

Above relations (Eqs. (19a-d) - (20a-d)) are used for evaluating \mathcal{P}^\pm (Eq. (14)) and \mathcal{B}^\pm (Eq. (15)). These results are further used in estimating p_d^\pm . Finally, the predicted values of p_d^\pm are used in expression for Δ (Eq. (12)) to find the analytical estimate for acoustic energy absorption coefficient in conical ducts with linear temperature gradient.

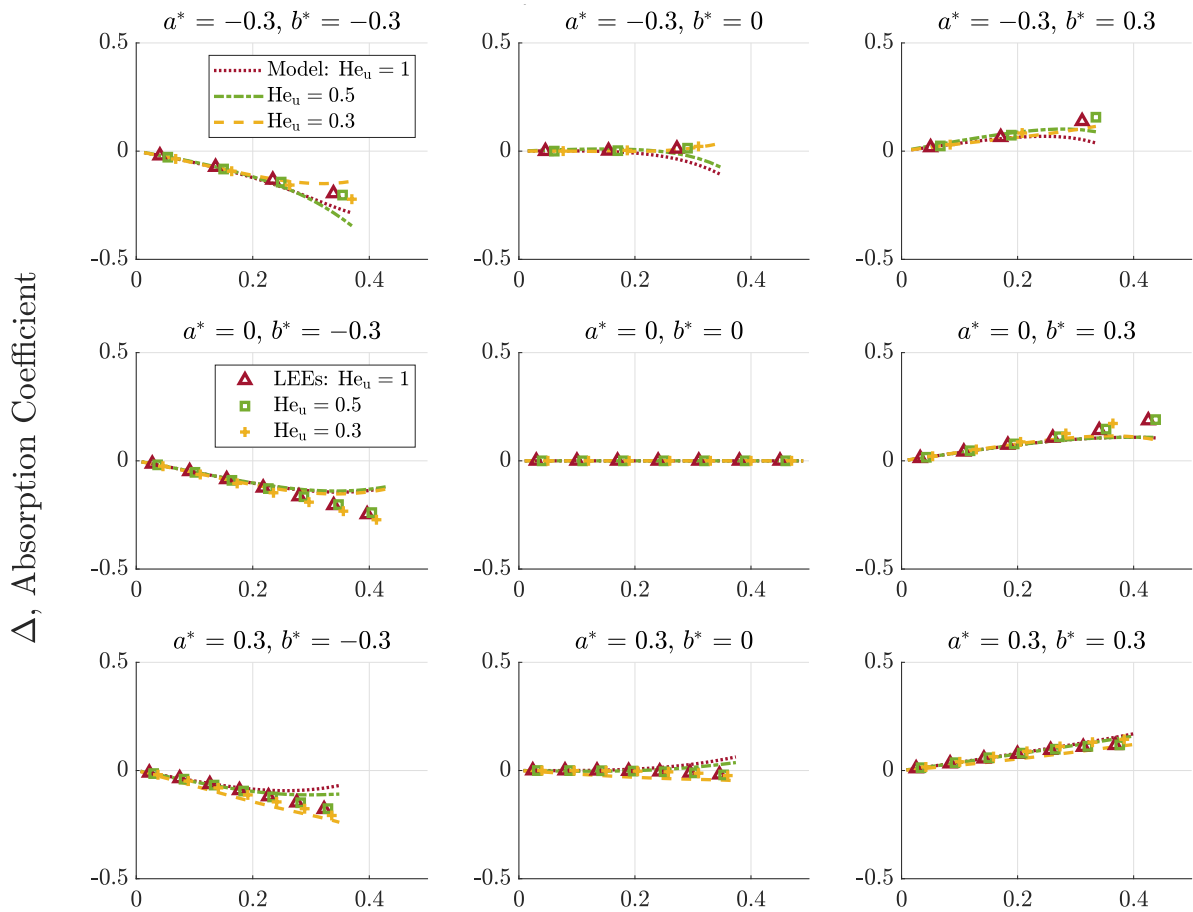
5. RESULTS

Fig. 2 compares the numerical and analytical results of Δ obtained as a function of inlet Mach-number (M_u) and Helmholtz number (He_u) for an anechoic inlet boundary ($|R_u| = 0$). Three different values of a^* and b^* are chosen. In performing the simulation, the maximum flow Mach number in the duct is limited to 0.5 in this analysis. This restricts the value of M_{avg} (average of upstream and downstream Mach-numbers) in the plots. For an anechoic boundary upstream, it can be observed that both the



$$M_{avg} = (M_u + M_d) / 2, \text{ average Mach number}$$

Figure 2: Comparison of Δ obtained analytically and numerically (for Helmholtz number = 1) as a function of inlet Mach number M_u , for a conical duct with anechoic inlet boundary ($|R_u| = 0$) and a linear temperature gradient. In the plots, the value of area coefficient (a^*) is varied from top to bottom, and temperature variation coefficient b^* is varied from left to right.



$$M_{avg} = (M_u + M_d) / 2, \text{ average Mach number}$$

Figure 3: Comparison of Δ obtained analytically and numerically (for Helmholtz number = 1) as a function of inlet Mach number M_u , for a conical duct with non-anechoic inlet boundary ($|R_u| = 0.5$) and a linear temperature gradient. In the plots, the value of area coefficient (a^*) is varied from top to bottom, and temperature variation coefficient b^* is varied from left to right.

numerical and analytical results do not change with the Helmholtz number. When M_{avg} is less than 0.25, the analytical estimate of acoustic energy absorption coefficient (Δ) is accurately captured.

In the regimes of low Mach number, where the model is accurate, the effect of temperature variation (b^*) can be seen to have a stronger influence on Δ , compared to area variation. When the temperature variation parameter changes sign from -0.3 to 0.3 , Δ also changed its sign. This implies, as the flow Mach-numbers increase there is an increase in acoustic generation for negative b^* and acoustic absorption increases with flow Mach numbers when b^* is positive. However, no such trend can be noticed for the area variation parameter a^* suggesting a weaker dependence.

Similarly, Fig. 3 compares the analytical and numerical results of Δ for a non-anechoic boundary condition at the inlet (with $|R_u| = 0.5$). While the numerical estimates still behave as frequency independent, the analytical model slightly deviates at low values of inlet Helmholtz number, ($He = 0.3$). This can be attributed to the fact that semi-analytical solution works poorly when the frequencies are decreased [7, 10]. However, when the average of flow Mach-numbers at inlet and outlet is less than 0.25, the analytical estimate still matches correctly to the numerical result.

6. CONCLUSIONS

This paper presents an analytical solution for estimating acoustic energy absorption coefficient in a varying area duct sustaining a non-isentropic mean flow. Firstly, a numerical mechanism is developed by recasting the linearised Euler equations into a system of first order differential equations in terms of positive (+) and negative (-) direction propagating planar wave amplitudes along with the entropy wave. Using a low Mach-number assumption, typical for combustors, the effect of acoustic-entropy coupling is neglected. Once the system of equations are solved for wave amplitudes at the downstream end, Δ is evaluated numerically. Similarly, a semi-analytical solution is used to estimate the acoustic field inside the duct from which Δ is analytically predicted. For different flow and area configurations the numerical and analytical results are compared, and it was found that the analytical estimates were accurate, provided the low frequency limit of the semi-analytical solution is satisfied and average of upstream and downstream Mach numbers is less than ~ 0.25 . It was also found that the results were independent of frequency and temperature variation along the duct has a stronger influence on Δ when compared to area variation.

7. ACKNOWLEDGEMENTS

The authors would like to acknowledge the European Research Council (ERC) Consolidator Grant AFIRMATIVE (2018-2023) and Inlaks Shivdasani foundation for supporting the current research.

8. REFERENCES

- [1] Dowling AP, Stow SR. Acoustic analysis of gas turbine combustors. *Journal of propulsion and power*. 2003 Sep;19(5):751-64.
- [2] Poinot T, Veynante D. *Theoretical and numerical combustion*. RT Edwards, Inc.; 2005.
- [3] Howe MS. Attenuation of sound in a low Mach Number nozzle flow. *Journal of Fluid Mechanics*. 1979 Mar;91(2):209-29.
- [4] Heywood JB. *Combustion engine fundamentals*. 1^a Edição. Estados Unidos. 1988.
- [5] Dokumaci E. An approximate analytical solution for plane sound wave transmission in inhomogeneous ducts. *Journal of sound and vibration*. 1998 Nov 12;217(5):853-67.
- [6] Xia Y, Duran I, Morgans AS, Han X. Dispersion of entropy perturbations transporting through an industrial gas turbine combustor. *Flow, turbulence and combustion*. 2018 Mar 1;100(2):481-502.
- [7] Yeddula SR, Morgans AS. A semi-analytical solution for acoustic wave propagation in varying area ducts with mean flow. *Journal of Sound and Vibration*. 2020 Oct 3;115770.
- [8] Gaudron R, Morgans AS. Acoustic absorption in a subsonic mean flow at a sudden cross section area change. In *Proceedings of ICSV 26—International Congress on Sound and Vibration 2019* (pp. 1-8).
- [9] Gaudron R, Yang D, Morgans AS. Acoustic energy balance during the onset, growth and saturation of thermoacoustic instabilities, *Journal of engineering for gas turbines and power*, 2020-16158.
- [10] Li J, Morgans AS. The one-dimensional acoustic field in a duct with arbitrary mean axial temperature gradient and mean flow. *Journal of Sound and Vibration*. 2017 Jul 21;400:248-69.